# Binding of Gold Clusters with DNA Base Pairs: A Density Functional Study of Neutral and Anionic GC−$Au_n$ and AT−$Au_n$ ($n$ = 4, 8) Complexes

**Anil Kumar,[†] P. C. Mishra,[†] and Sándor Suhai*[,‡]**

*Department of Physics, Banaras Hindu University, Varanasi-221 005, India, and Department of Molecular Biophysics, Deutsches Krebsforschungszentrum, Im Neuenheimer Feld 580, 69120 Heidelberg, Germany*

*Received: February 13, 2006; In Final Form: April 11, 2006*

Binding of clusters of gold atoms (Au) with the guanine−cytosine (GC) and adenine−thymine (AT) Watson−Crick DNA base pairs was studied using the density functional theory (DFT). Geometries of the neutral GC−$Au_n$ and AT−$Au_n$ and the corresponding anionic $(GC-Au_n)^{-1}$ and $(AT-Au_n)^{-1}$ ($n$ = 4, 8) complexes were fully optimized in different electronic states, that is, singlet and triplet states for the neutral complexes and doublet and quartet states for the anionic complexes, using the B3LYP density functional method. The 6-31+G** basis set was used for all atoms except gold. For gold atoms, the Los Alamos effective core potential (ECP) basis set LanL2DZ was employed. Vibrational frequency calculations were performed to ensure that the optimized structures corresponded to potential energy surface minima. The gold clusters around the neutral GC and AT base pairs have a T-shaped structure, which satisfactorily resemble those observed experimentally and in other theoretical studies. However, in anionic GC and AT base pairs, the gold clusters have extended zigzag and T-shaped structures. We found that guanine and adenine have high affinity for Au clusters, with their N3 and N7 sites being preferentially involved in binding with the same. The calculated adiabatic electron affinities (AEAs) of the GC−$Au_n$ complexes ($n$ = 4, 8) were found to be much larger than those of the isolated base pairs.

## Introduction

Nanometer scale DNA-based device technology is an attractive option due to the special properties of DNA, for example, recognition, self-assembly, specificity of binding with metals, and the fact that its structure can be controlled by the incorporation of different sequences of base pairs.[1,2] While the conductive or charge transport behavior of native DNA suffers from controversy,[3] it is established that metal-bound DNA nanowires have substantial conductivity.[4,5] Recently, it has become an active area of research, and fabrication of metallic nanowires combined with DNA obtained by chemical deposition of thin metallic films, especially those of gold, onto DNA has been carried out.[3−5] The sequence-specific hybridization and replication properties of DNA have been used for self-assembly of nanostructures and for highly sensitive detection.[6−8] Presently, most experimental and theoretical investigations are focused on gold-molecule−gold-transport junctions.[9] In this context, the basic question as to how binding occurs between DNA and gold should be answered.

The charge transport properties of DNA are of central importance in the development of devices.[3,4] A link between oxidative damage of DNA due to hole transfer and the occurrence of genetic mutation has been established.[5,8b] It is established that guanine plays a crucial role in charge transport processes in DNA because of its lowest ionization potential.[10] It is also found that acquisition of excess electronic charge by DNA leads to various modifications of its chemical and physical properties.[10c] By the use of both experimental and theoretical methods, attempts have been made to unravel the mechanism of charge transfer within DNA.[10c] Giese et al.[11] measured the efficiency of charge transfer between guanines separated by different numbers of AT base pairs and found that it depends on the distance between them. Using photodetachment-photoelectron spectroscopy (PD-PES), Schiedt et al.[12] obtained electron affinities (EAs) of nucleic acid bases bases T, C, and U in the presence of water clusters and found the EAs to be positive. Wetmore et al.[13] also reported positive EAs of the nucleic acid bases using the B3LYP/6-31+G(d,p) level of theory. Adamowicz and co-workers[14] proposed a "dipole bound anion" for DNA bases while Bowen and co-workers[15] found that microsolvation of anionic uracil with even a single water molecule sufficiently stabilizes the system to accommodate the excess electron. Schuster et al.[16] studied charge migration in a hydrated B-DNA duplex and proposed an ion-gated charge-transfer mechanism for DNA. The gas-phase EAs of DNA bases and base pairs have been extensively studied by Schaefer and co-workers,[17] Wiley et al.,[18] Chen et al.,[19] Sevilla and co-workers,[20] and Gutowski et al.[21] using theoretical and experimental methods. Recently, we used an empirical density functional (SCC-DFTB) method[22a] to compute adiabatic electron affinities (AEAs) of GC, AT, and hypoxanthine (HX)−C base pairs in the gas phase and those of hydrated AT[22b] and GC[22c] base pairs at the B3LYP/6-31+G** level of theory. We found that hydrated base pairs have higher EAs than the corresponding gas-phase systems. Developments in this area have been reviewed recently.[2e,5b,8b,23,24] DNA−metal, particularly DNA−gold, complexes appear to be good candidates for investigation of properties relevant to their use in nanobiotechnology.[2a,2d,6,8b,25−34] The binding of clusters of three and six gold atoms, from the catalytic point of view of Au particles, to the individual DNA bases and Watson−Crick

* To whom correspondence should be addressed. E-mail: mol.biophys@dkfz.de.
[†] Banaras Hindu University.
[‡] Deutsches Krebsforschungszentrum.

10.1021/jp060932a CCC: $33.50 
Published on Web 05/25/2006

AT and GC base pairs employing triangular T-shaped geometries was studied recently.[34]

We have addressed ourselves here the question as to what are the geometries, stabilities, and properties of the neutral and anionic complexes of DNA bases and base pairs with clusters of four or eight gold atoms each. In the present study, we considered four and eight gold atoms due to two reasons: (i) we considered four gold atoms since a recent molecular dynamics ab initio study[28] showed that the optimal size of a gold nanowire that can be formed is about 11 Å in length, which would consist of three to four bonded gold atoms, and (ii) we considered eight gold atoms because a comparison of the results obtained with it with those obtained with four gold atoms would reveal information as to how the binding properties of gold clusters would change when the number of gold atoms is appreciably increased. It is known from experimental studies[35] that the reactivity of gold arises due to the presence of low coordinated gold atoms. We have included in this study the anions of complexes of gold clusters with the AT and GC base pairs since it would reveal information relevant to transfer or flow of charge during electrical conduction. As electron density distributions and electron affinities are important properties in this context, these have been studied in detail. It may be noted that anionic complexes of the DNA bases and base pairs with gold clusters and their electron affinities have not been studied before.

**Method of Calculations.** Geometries of the GC and AT base pairs in their neutral and anionic forms complexed with four and eight gold atoms each were fully optimized using the B3LYP form of density functional theory (DFT). The B3LYP density functional is a combination of Becke's three-parameter hybrid exchange functional[36,37] and the Lee−Yang−Parr[38] correlation functional. The B3LYP hybrid functional includes the exchange functional as a linear combination of Hartree−Fock, local, and gradient-corrected exchange terms. We used the 6-31+G** basis set for all the atoms except gold. For gold, we used the Los Alamos effective-core potential (ECP) Lanl2DZ basis set.[39] In this basis set, [Xe]4f inner electrons of Au are used while the 11 outermost electrons are explicitly described using a double-$\zeta$ basis set. The mixed basis set used here will be denoted by 6-31+G**∪Lanl2DZ. Vibrational frequencies were calculated for all the optimized systems, and real frequencies were obtained in all the cases. In the present calculations, the Gaussian 03 suite of programs was employed.[40] The electronic isodensity surfaces of some molecular orbitals were plotted using the GaussView program.[41]

## Results and Discussion

The starting geometries of neutral and anionic AT−$Au_n$ and GC−$Au_n$ ($n = 4, 8$) complexes for optimization were generated by placing two or four gold atoms, four or eight in total, in each case, near the electron-rich sites of the AT and GC base pairs (Figures 1 and 2). The B3LYP/6-31+G**∪Lanl2DZ optimized structures of the neutral and anionic AT base pairs complexed with four gold atoms each are shown in parts a and b of Figure 1, respectively, while the corresponding structures for the GC base pair are shown in parts a and b of Figure 2, respectively. The electronic state of each of the optimized structures of the neutral AT−$Au_4$ and GC−$Au_4$ complexes was singlet while the electronic state of each of the corresponding anionic complexes was doublet. The neutral AT−$Au_4$ complex in the singlet state was found to be more stable than in the corresponding triplet state by ∼2.2 eV while the anionic AT−$Au_4$ complex in the doublet state was found to be more stable than in the quartet state by ∼1.8 eV. The neutral GC−$Au_4$ complex in the singlet state was found to be more stable than in the triplet state by ∼2.4 eV while the anionic GC−$Au_4$ complex in the doublet state was found to be more stable than in the quartet state by ∼2.3 eV. Due to this reason, properties of the neutral AT−$Au_4$ and GC−$Au_4$ complexes in the triplet states and those of the anionic AT−$Au_4$ and GC−$Au_4$ complexes in the quartet states are not presented here. Further, for the same reason, the structures of neutral AT−$Au_8$ and GC−$Au_8$ complexes were optimized in the corresponding singlet states while those of the corresponding anionic complexes were optimized in the corresponding doublet states only (Figure 3).

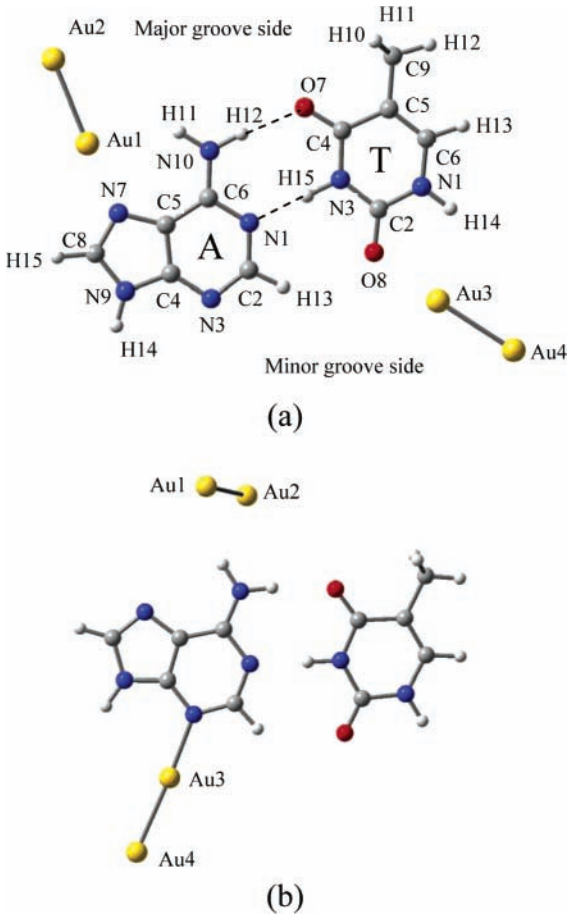


**Figure 1.** Optimized structures of neutral and anionic AT−$Au_4$ in singlet (a) and doublet (b) states, respectively, obtained at the B3LYP/6-31+G**∪Lanl2DZ level of theory. Parts a and b have the same numbering scheme.

Plots of electronic isodensity surfaces of the highest occupied molecular orbital (HOMO) and lowest unoccupied molecular orbital (LUMO) in the singlet state of neutral AT−$Au_8$ and singly occupied molecular orbital (SOMO) of anionic AT−$Au_8$ in the doublet state are presented in parts a, b, and c of Figure 4, respectively, while the corresponding plots for the neutral and anionic GC−$Au_8$ complexes are presented in Figure 5, respectively. Some selected geometrical parameters of the optimized neutral and anionic AT−$Au_n$ ($n = 4, 8$) complexes are presented in Table 1 while the corresponding results for the neutral and anionic GC−$Au_n$ ($n = 4, 8$) complexes are presented in Table 2. The hydrogen bonding distances in the AT−$Au_4$ and GC−$Au_4$ complexes are given in Table 3. The net charge distributions calculated using the Mulliken population scheme in the neutral and anionic AT−$Au_8$ and GC−$Au_8$ complexes are presented in Tables 4 and 5, respectively. The calculated

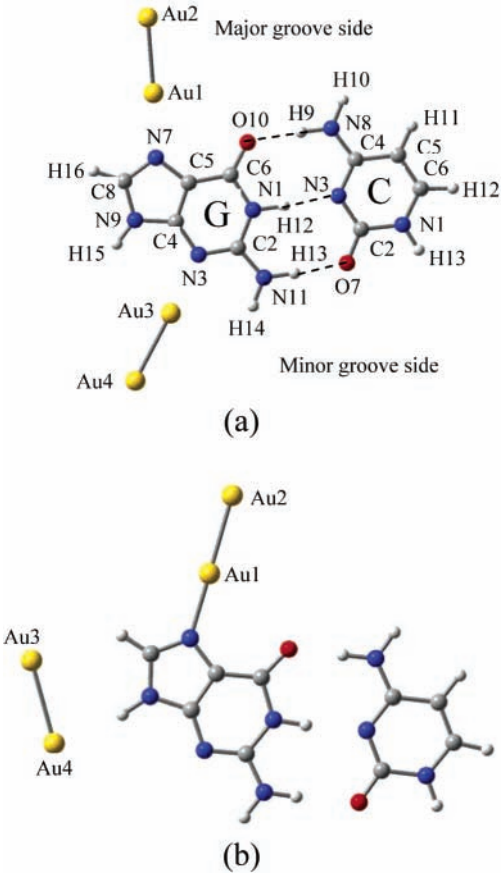


**Figure 2.** Optimized structures of neutral and anionic GC−$Au_4$ in singlet (a) and doublet (b) states, respectively, obtained at the B3LYP/6-31+G**∪Lanl2DZ level of theory. Parts a and b have the same numbering scheme.

AEAs of the neutral AT−$Au_n$ and GC−$Au_n$ ($n$ = 4, 8) complexes are presented in Table 6.

**Structures of Neutral Complexes.** A comparison of the hydrogen bonding distances in the normal Watson−Crick AT and GC base pairs with those in the AT−$Au_n$ and GC−$Au_n$ ($n$ = 4, 8) complexes would be interesting. The hydrogen bonding distances in the neutral base pairs have also been obtained experimentally.[42−45] In crystals of sodium adenylyl-3′,5′-uridine hexahydrate,[44] the hydrogen bonding distances N10(A)−O7(T) and N1(A)−N3(T) were observed to be 2.95 and 2.82 Å, respectively (Figure 1). The corresponding distances calculated using theory at the B3LYP/6-31+G**∪Lanl2DZ level for the singlet state of neutral AT−$Au_4$ were found to be 2.949 and 2.851 Å (Table 3). In the AT−$Au_8$ complex, the calculated N10(A)−O7(T) and N1(A)−N3(T) hydrogen bonding distances are increased by ∼0.02 and ∼0.08 Å, respectively, with respect to those in the AT−$Au_4$ complex (Table 3). The hydrogen bonding distances O10(G)−N8(C), N1(G)−N3(C), and N11(G)−O7(C) in the neutral GC base pair (Figure 2) were found to be 2.91, 2.95, and 2.86 Å by X-ray crystallography.[45] The values of these distances obtained by us are 2.846, 2.900, and 2.820 Å in GC−$Au_4$ and 2.824, 2.860, and 2.790 Å in GC−$Au_8$. Thus, we find that the hydrogen bonding distances are all decreased when going from GC−$Au_4$ to GC−$Au_8$ (Table 2), that is, opposite to what is found in the AT−$Au_4$ and AT−$Au_8$ complexes (Table 1). These results show that, broadly speaking, the hydrogen bond lengths in the base pairs are increased or decreased due to their complexation with gold clusters. Recently, Kurita et al.[46] optimized geometries of the AT and GC base pairs at the MP2 level with several basis sets and found that, depending on the basis set used, the hydrogen bond lengths were shortened by 0.10−0.15 Å in the AT base pair and 0.06−0.11 Å in the GC base pair in comparison to those obtained at the Hartree−Fock level. They argued that the calculated shortening of hydrogen bond lengths was due to the dispersion attraction.[46] Their optimized GC base pair was somewhat nonplanar while the AT base pair had a planar ring structure.[46] We also find that the neutral and anionic complexes of the AT base pair with gold clusters are planar. Further, the neutral complexes of the GC base pair with gold clusters are planar while the anionic GC−$Au_8$ complex is slightly nonplanar.

In the neutral AT−$Au_4$ complex, in the singlet state, a pair of gold atoms was found to be located near the N7 and O8 sites of the adenine and thymine moieties, respectively (Figure 1a). The optimized Au1−Au2, Au3−Au4, Au1−N7(A), and Au3−O8(T) distances were found to be 2.565, 2.560, 2.160, and 2.260 Å, respectively (Table 1). The binding of eight gold atoms around the AT base pair in the singlet state is shown in Figure 3a. In the optimized AT−$Au_8$ complex, the gold atoms are clustered in two groups, one near the N7 atom of adenine and the other near the N3 atom of the same molecule (Figure 3a). Further, in each subgroup, three gold atoms are located at the corners of a triangle forming a T-shaped structure in each case. In the AT−$Au_8$ complex, the distances Au1−Au2, Au2−Au3, Au3−Au4, and Au1−Au3 were found to be 2.635, 2.740, 2.590, and 2.860 Å, respectively, while the distances Au5−Au6, Au6−Au7, Au7−Au8, and Au5−Au7 were found to be 2.630, 2.740, 2.600, and 2.860 Å, respectively (Figure 3a, Table 1). The distances Au1−N7(A) and Au5−N3(A) (Figure 3a) were found to be 2.140 and 2.130 Å, respectively. Recently, Kryachko and Remacle[34] carried out a theoretical study of the binding of gold atoms employing triangular and T-shaped structures, with the isolated DNA bases A, T, G, and C as well as AT and GC base pairs at the B3LYP/RECP(gold)∪6-31++G(d,p) and B3LYP/RECP(gold)∪6-31+G(d) levels of theory. These authors calculated the binding of gold clusters with the bases and found that $Au_3$ preferentially bound to the N1, N3, and N7 sites of the adenine and O7 and O8 sites of thymine (Figure 1). In their study,[34] the Au−N bond lengths were found to lie in the range 2.130−2.153 Å, while the Au−O bond lengths were found to lie in the range 2.177−2.239 Å. The T-shaped $Au_4$ gold cluster binds with the N3 side of the adenine extending toward the N9 side.[34] Also, in the AT−$Au_3$ complex, they found the N3 and N7 sites of adenine to be most favorable for the binding of gold clusters.[34] As in our case, they also found that the binding of $Au_3$ with thymine was less stable, which is in agreement with the experimental observation by Lindsay and co-workers.[47] Using scanning electron microscopy (SEM), atomic force microscopy (AFM), and cyclic voltammetry, Lindsay and co-workers[47] studied the adsorption of DNA bases A, T, G, and C on the Au(111) surface and found that A, G, and C were adsorbed on the Au electrode but T was not. The calculated Au5−Au6, Au6−Au7, Au7−Au8, and Au5−Au7 bond lengths in the previous work[34] were found to be 2.623, 2.708, 2.593, and 2.823 Å, respectively, which agree very well with our calculated bond lengths (Table 1).

A cluster of four gold atoms preferentially binds with the N3 and N7 sites of guanine of the neutral GC base pair in the singlet state (Figure 2a). The optimized Au1−Au2, Au3−Au4, and Au1−N7 and Au3−N3 bond distances at the B3LYP/6-31+G**∪Lanl2DZ level of theory were found to be 2.571, 2.550, 2.160, and 2.190 Å, respectively (Table 2). The gold clusters in the neutral GC−$Au_8$ complex are also located near the N3 and N7 sites of guanine in a manner similar to what is

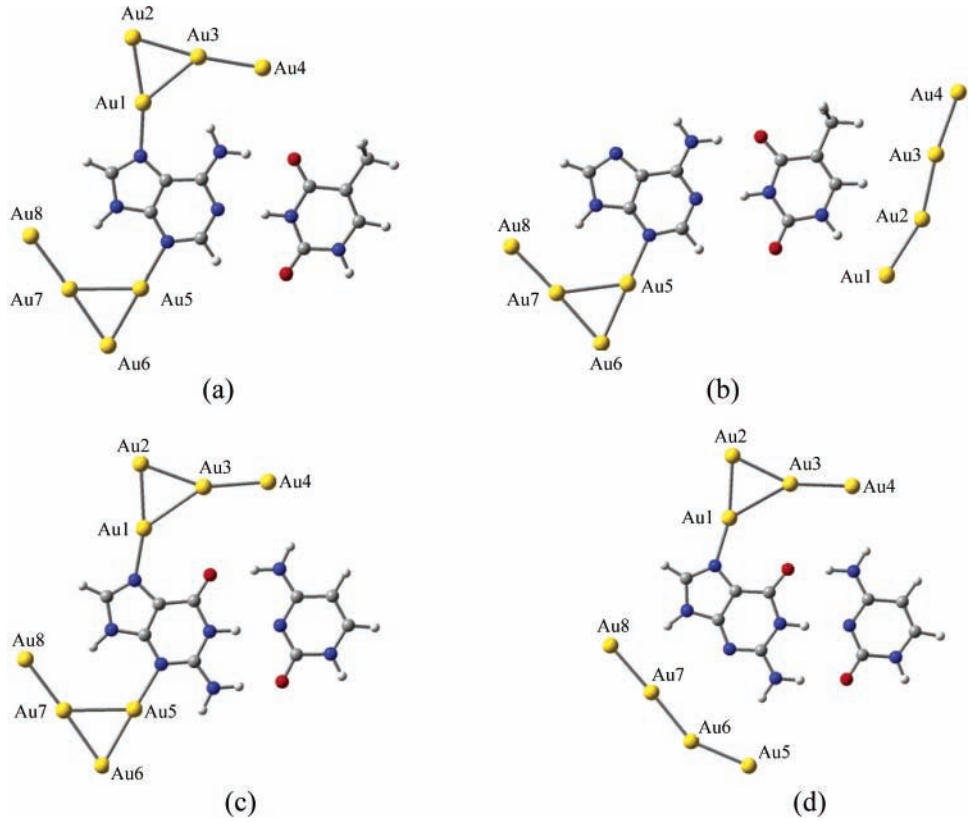


**Figure 3.** Optimized structures of neutral and anionic AT−$Au_8$ complexes in singlet (a) and doublet (b) states and GC−$Au_8$ complexes in singlet (c) and doublet (d) states, respectively, obtained at the B3LYP/6-31+G**∪Lanl2DZ level. Numbering schemes for AT and GC base pairs are the same as those in Figures 1 and 2.

found in the neutral AT−$Au_8$ complex (parts a and c of Figure 3). The bond distances Au1−Au2, Au2−Au3, Au3−Au4, and Au1−Au3 in the GC−$Au_8$ complex were found to be 2.632, 2.720, 2.620, and 2.950 Å, respectively, while the Au5−Au6, Au6−Au7, Au7−Au8, and Au5−Au7 distances were found to be 2.628, 2.740, 2.600, and 2.860 Å, respectively. Our Au−N distances in both the AT−$Au_8$ and GC−$Au_8$ complexes lie between 2.130 and 2.155 Å (Tables 1 and 2). The corresponding bond distances obtained by Kryachko and Remacle[34] lie in the range 2.131−2.138 Å. Thus, the present and previously[34] calculated Au−N bond distances are in a good agreement. The complexes of the $Au_3$ gold cluster located near the N3 and N7 sites of the GC base pair calculated at the B3LYP/RECP-(gold)∪6-31+G(d) level of theory were found to have binding energies 19.3 and 18.0 kcal/mol, respectively.[34b] Recently, Giese and McNaughton[48] studied the interaction of guanine, 7-methylguanine (7-MetG), and 9-ethylguanine (9-EtG) on the silver surface using surface-enhanced Raman spectroscopy (SERS) and DFT. They found that guanine and 7-MetG were absorbed on the silver surface such that their N11−N3−C4−N9 side was directed toward the silver surface while 9-EtG was adsorbed with the N7−C6−O10 side directed toward the same (Figure 2).

**Structures of Anionic Complexes.** The anions of AT−$Au_n$ and GC−$Au_n$ ($n$ = 4, 8) were generated by adding an excess electron to each of the neutral complexes. Different binding patterns of gold clusters in the anionic complexes from those in the corresponding neutral complexes were obtained (Figures 1b, 2b, 3b, and 3d). In the anionic AT−$Au_4$ complex in the doublet state (Figure 1b), two gold atoms are bound near the N3 site of adenine while the other two gold atoms are located near the $NH_2$ group of the same moiety. In this case, the Au1−Au2, Au3−Au4, and Au3−N3 bond lengths were found to be 2.733, 2.580, and 2.140 Å, respectively. In the case of the anionic AT−$Au_8$ complex in the doublet state (Figure 3b), the binding pattern is strongly modified in comparison with that in the corresponding neutral complex. Thus, the cluster of the gold atoms Au1, Au2, Au3, and Au4 that binds to the N7 site of adenine in the neutral AT−$Au_8$ complex adopts an extended, zigzag conformation and gets shifted to near the C5, C6, N1 side of thymine in the corresponding anionic complex (parts a and b of Figure 3). However, the cluster of Au5, Au6, Au7, and Au8 atoms of gold remains bound near the N3 site of adenine when going from the AT−$Au_8$ complex to the corresponding anionic complex (parts a and b of Figure 3). The Au−Au bond lengths are usually increased or decreased by ∼0.01−0.10 Å when going from the neutral AT−$Au_8$ to the corresponding anionic complex (Tables 1). The hydrogen bonding distance N10(A)−O7(T) is decreased by ∼0.16 Å while the N1(A)−N3(T) distance is increased by ∼0.05 Å when going from the neutral AT−$Au_8$ complex to the corresponding anionic complex (Table 3). Similar trends of changes in hydrogen bond lengths in anionic AT and GC base pairs have been found earlier by us[22a] and others.[17b] Through the use of different theoretical methods,[22a,17b] a substantial nonplanarity in the thymine moiety in an anionic AT base pair has been found, while in the anionic AT−$Au_n$ ($n$ = 4, 8) complex, the thymine moiety is planar.

The binding of clusters of four and eight gold atoms to the anionic GC base pair is shown in Figures 2b and 3d, respectively. In the anionic GC−$Au_4$ complex in the doublet state, the gold atoms Au1 and Au2 are bonded together and Au1 is bound to the N7 atom of guanine while Au3 and Au4 are bonded together and are located near the C8, N9 sites of guanine. With respect to the neutral GC−$Au_8$ complex, a large structural change occurs in the corresponding anionic complex in the binding pattern of gold atoms near the N3 site of guanine (parts

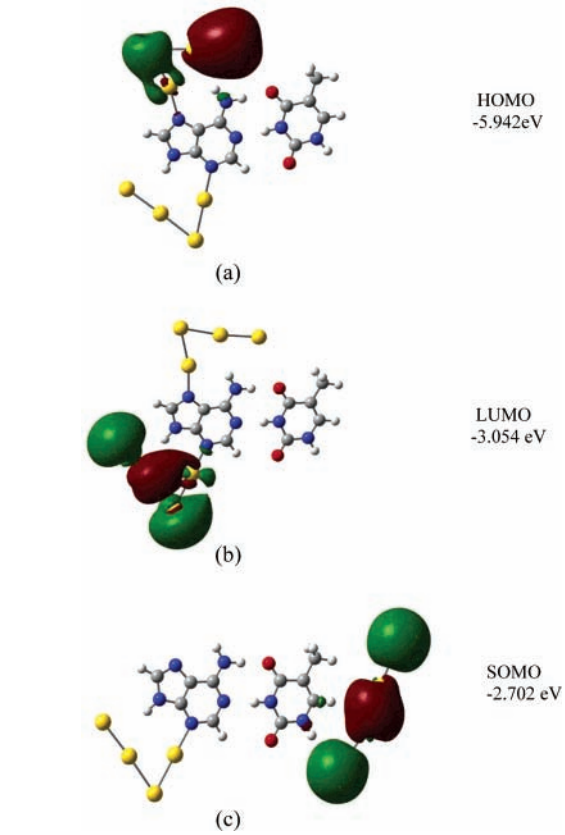


**Figure 4.** Isodensity surfaces of the (a) highest occupied molecular orbital (HOMO) and (b) lowest unoccupied molecular orbital (LUMO) for the neutral AT−$Au_8$ complex and (c) singly occupied molecular orbital (SOMO) for the anionic AT−$Au_8$ complex. The corresponding orbital energies are also given.

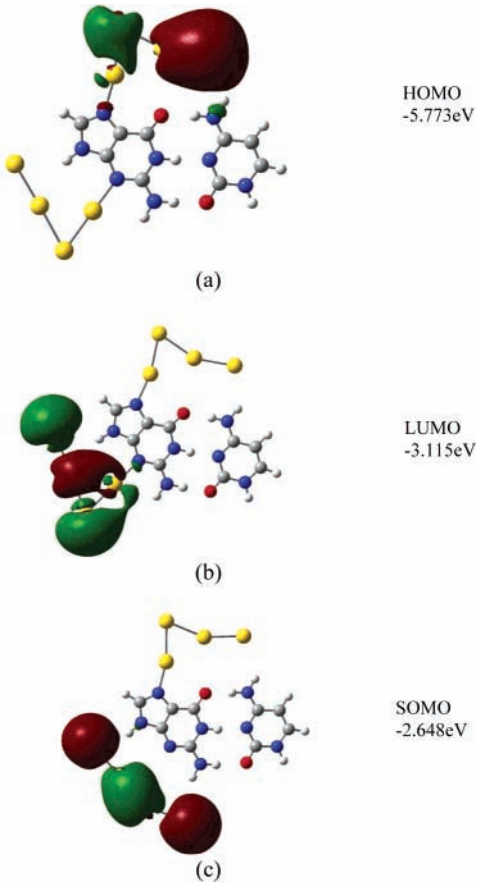


**Figure 5.** Isodensity surfaces of (a) the highest occupied molecular orbital (HOMO) and (b) lowest unoccupied molecular orbital (LUMO) for the neutral GC−$Au_8$ complex and (c) singly occupied molecular orbital (SOMO) for the anionic GC−$Au_8$ complex. The corresponding orbital energies are also given.

c and d of Figure 3). Thus, while the cluster of Au1, Au2, Au3, and Au4 atoms is bound near the N7 site of guanine in both the neutral and anionic GC−$Au_8$ complexes without a change in shape, the cluster of Au5, Au6, Au7, and Au8 adopts an extended, zigzag conformation and remains bound near the N3 site of guanine (parts c and d of Figure 3). We find that the gold clusters bound to adenine and guanine change differently when going from the neutral to the corresponding anionic AT−$Au_n$ and GC−$Au_n$ ($n$ = 4, 8) complexes. The Au−Au distances lie between 2.620 and 2.950 Å in the anionic GC−$Au_8$ complex (Table 2). The hydrogen bonding distances O10(G)−N8(C) and N11(G)−O7(C) in the anionic GC−$Au_n$ ($n$ = 4, 8) complexes are appreciably decreased and increased, respectively, as compared with those in the corresponding neutral complexes.

In the neutral AT−$Au_8$ complex, we found that the Au1−Au2−Au3−Au4 cluster adopts a planar structure while the Au5−Au6−Au7−Au8 cluster has a small nonplanarity (∼8°). However, in the anionic AT−$Au_8$ complex, both the corresponding clusters have planar structures (Table 1 and parts a and b of Figure 3). In both the neutral and anionic GC−$Au_8$ complexes, the clusters Au1−Au2−Au3−Au4 and Au5−Au6−Au7−Au8 were found to be planar except that the Au5−Au6−Au7−Au8 cluster in anionic GC−$Au_8$ is nonplanar by ∼18°. In a recent study,[49] the property of gold atoms favoring planar structures up to 13 atoms was correlated with relativistically enhanced hybridization between s- and d-type orbitals and d−d interactions. We also found that gold clusters in neutral and anionic complexes were stabilized due to long-range interactions[34] between atoms separated by 2.552−2.992 Å (Tables 1 and 2). Certain vibrational frequencies of neutral and anionic GC−$Au_8$ and AT−$Au_8$ complexes provide information about differences in their behavior. For example, we found that when going from a neutral to anionic AT−$Au_8$ complex, the stretching frequency $\nu$(N10(A)−H12(A)) is red shifted by ∼163 $cm^{-1}$ while the stretching frequency $\nu$(N3(T)−H15(T)) is blue shifted by ∼118 $cm^{-1}$. In the GC−$Au_8$ complex, when going from the neutral to the anionic complex, the stretchings frequencies $\nu$(N11(G)−H13(G)) and $\nu$(N1(G)−H12(G)) are blue shifted by ∼286 and 235 $cm^{-1}$, respectively, while the stretchings frequency $\nu$(N8(C)−H9(C)) is red shifted by ∼127 $cm^{-1}$.

**Electronic Charge Distribution.** A detailed analysis of charge distributions in the neutral and anionic AT−$Au_8$ and GC−$Au_8$ complexes was carried out using the Mulliken population analysis scheme. The charge distributions for neutral and anionic AT−$Au_8$ complexes are given in Table 4. In the neutral AT−$Au_8$ complex, we find that adenine loses a substantial amount of negative charge (−0.580 e, where e is the magnitude of the electronic charge), the thymine moiety gains a little amount of negative charge (−0.016 e) while the gold clusters gain appreciable amount of negative charge (−0.565 e) (Table 4). In the anionic AT−$Au_8$ complex, a large amount of negative charge (−1.565 e) is localized on gold atoms Au1−Au8 while both the adenine and thymine moieties lose negative charges (−0.294 and −0.271 e, respectively) (Table 4). In the neutral GC−$Au_8$ complex (Table 5), according to the Mulliken charge distributions, the guanine and cytosine moieties lose −0.490 and −0.100 e charges, respectively, whereas gold clusters Au1−Au8 gain the same (−0.589 e). In the anionic

**TABLE 1: Some Selected Geometrical Parameters (angstroms, degrees) of Fully Optimized Neutral (singlet state) and Anionic (doublet state) AT−$Au_4$ and AT−$Au_8$ Complexes Obtained at the B3LYP/6-31+G**∪Lanl2DZ Level[a]**

| | AT−$Au_4$ and state | | AT−$Au_8$ and state | |
|---|---|---|---|---|
| geometrical parameters | singlet | doublet | singlet | doublet |
| Bond Lengths | | | | |
| Au1−Au2 | 2.565 | 2.733 | 2.635 | 2.669 |
| Au2−Au3 | | | 2.740 | 2.690 |
| Au3−Au4 | 2.560 | 2.580 | 2.590 | 2.660 |
| Au1−Au3 | | | 2.860 | |
| Au5−Au6 | | | 2.630 | 2.640 |
| Au6−Au7 | | | 2.740 | 2.640 |
| Au7−Au8 | | | 2.600 | 2.610 |
| Au5−Au7 | | | 2.860 | 2.830 |
| Au1−N7(A) | 2.160 | 4.440 | 2.140 | |
| N10(A)−C6(A) | 1.330 | 1.320 | 1.320 | 1.330 |
| N3(A)−Au3 | | 2.140 | | |
| Au5−N3(A) | | | 2.130 | 2.120 |
| Au3−O8(T) | 2.260 | | | |
| C4(T)−O7(T) | 1.230 | 1.230 | 1.230 | 1.240 |
| C2(T)−O8(T) | 1.250 | 1.220 | | 1.220 |
| Au3−H11(A) | | | 2.891 | |
| Au7−H14(A) | | | 2.823 | 2.992 |
| Au8−H14(A) | | | 2.754 | 2.877 |
| Au1−H14(T) | | | | 2.566 |
| Au2−H13(T) | | | | 2.804 |
| N10(A)−H11(A) | | | 1.015 | 1.009 |
| N10(A)−H12(A) | | | 1.028 | 1.036 |
| Bond Angles | | | | |
| Au1−Au2−Au3 | | | 64.7 | 160.0 |
| Au2−Au3−Au4 | | | 173.3 | 172.3 |
| N7(A)−Au1−Au2 | 177.9 | 93.5 | 168.3 | |
| Au1−N7(A)−C8(A) | 126.1 | 154.7 | | |
| Dihedral Angles | | | | |
| Au2−Au1−N7(A)−C8(A) | 176.3 | −113.8 | | |
| C6(A)−C5(A)−C4(A)−N9(A) | 180.0 | 180.0 | 180.0 | 180.0 |
| C4(A)−N3(A)−Au3−Au4 | | −6.4 | | |
| Au1−Au2−Au3−Au4 | | | 179.4 | 180.0 |
| N7(A)−Au1−Au2−Au3 | | | 180.0 | - |
| Au5−Au6−Au7−Au8 | | | −172.2 | 179.6 |
| N3(A)−Au5−Au6−Au7 | | | 177.4 | 179.4 |
| C2(A)−N1(A)−N3(C)−C4(T) | 180.0 | −178.1 | 179.0 | 180.0 |

[a] See Figure 1.

**TABLE 2: Some Selected Geometrical Parameters (angstroms, degrees) of Fully Optimized Neutral (singlet state) and Anionic (doublet state) GC−$Au_4$ and GC−$Au_8$ Complexes Obtained at the B3LYP/6-31+G**∪Lanl2DZ Level[a]**

| | GC−$Au_4$ and state | | GC−$Au_8$ and state | |
|---|---|---|---|---|
| geometrical parameters | singlet | doublet | singlet | doublet |
| Bond Lengths | | | | |
| Au1−Au2 | 2.571 | | 2.632 | 2.648 |
| Au2−Au3 | | | 2.720 | 2.710 |
| Au3−Au4 | 2.550 | 2.730 | 2.620 | 2.620 |
| Au1−Au3 | | | 2.950 | 2.950 |
| Au5−Au6 | | | 2.628 | 2.660 |
| Au6−Au7 | | | 2.740 | 2.690 |
| Au7−Au8 | | | 2.600 | 2.664 |
| Au5−Au7 | | | 2.860 | - |
| Au1−N7(G) | 2.160 | 2.130 | 2.155 | 2.127 |
| C6(G)−O10(G) | 1.230 | 1.240 | 1.220 | 1.243 |
| N3(G)−Au3 | 2.190 | 2.593 | | |
| Au5−N3(G) | | | 2.142 | |
| C4(C)−N8(C) | 1.330 | 1.330 | 1.330 | 1.332 |
| C2(C)−O7(C) | 1.240 | 1.230 | 1.240 | 1.238 |
| Au4−H10(C) | | | 2.788 | 2.883 |
| Au7−H15(G) | | | 2.846 | 2.903 |
| Au8− H15(G) | | | 2.789 | 2.552 |
| Au5−H14(G) | | | 2.762 | 2.931 |
| N11(G)−H14(G) | | | 1.010 | 1.014 |
| N11(G)−H13(G) | | | 1.036 | 1.020 |
| N8(C)−H9(C) | | | 1.026 | 1.034 |
| N8(C)−H10(C) | | | 1.014 | 1.012 |
| Bond Angle | | | | |
| Au1−Au2−Au3 | | | 66.9 | 66.9 |
| Au2−Au3−Au4 | | | 155.4 | 156.0 |
| N7(G)−Au1−Au2 | 177.8 | 179.6 | 167.4 | 166.2 |
| Au1−N7(G)−C8(G) | 124.3 | 127.2 | 129.6 | 129.7 |
| Dihedral Angle | | | | |
| Au2−Au1−N7(G)−C8(G) | −3.3 | −11.8 | −0.1 | 7.7 |
| C6(G)−C5(G)−C4(G)−N9(G) | 180.0 | 180.0 | 180.0 | 180.0 |
| C4(G)−N3(G)−Au3−Au4 | −5.9 | −0.5 | 1.5 | |
| Au1−Au2−Au3−Au4 | | | 180.0 | 178.0 |
| N7(G)−Au1−Au2−Au3 | | | 180.0 | 180.0 |
| Au5−Au6−Au7−Au8 | | | 180.0 | 162.7 |
| N3(G)−Au5−Au6−Au7 | | | 178.5 | - |
| C2(G)−N1(G)−N2(C)−C4(C) | 180.0 | 180.0 | 180.0 | 174.2 |

[a] See Figure 2.

**TABLE 3: Hydrogen Bond Lengths (angstroms) in the AT and GC Base Pairs in Their Neutral (singlet state) and Anionic (doublet state) AT−$Au_n$ and GC−$Au_n$ ($n$=2,4) Complexes Obtained at the B3LYP/6-31+G**∪Lanl2DZ Level[a]**

| hydrogen bond distances | state | | | | |
|---|---|---|---|---|---|
| | singlet | doublet | singlet | doublet | experiment[b] |
| | AT−$Au_4$ | | AT−$Au_8$ | | |
| N10(A)−O7(T) | 2.949 | 3.036 | 2.970 | 2.811 | 2.95 |
| N1(A)−N3(T) | 2.851 | 2.870 | 2.930 | 2.980 | 2.82 |
| | GC−$Au_4$ | | GC−$Au_8$ | | |
| O10(G)−N8(C) | 2.846 | 2.754 | 2.824 | 2.780 | 2.91 |
| N1(G)−N3(C) | 2.900 | 2.950 | 2.860 | 2.924 | 2.95 |
| N11(G)−O7(C) | 2.820 | 3.000 | 2.790 | 2.990 | 2.86 |

[a] For isolated base pairs. See Figures 1 and 2. [b] References 44 and 45.

GC−$Au_8$ complex, a large amount of negative charge (−1.414 e) is localized on the gold clusters while the guanine moiety loses an appreciable amount of negative charge (−0.404 e) and the cytosine moiety loses a small amount of negative charge (−0.009 e).

The charge distributions in the neutral and anionic complexes show that gold clusters are stabilized around AT and GC base pairs due to electrostatic interaction. In the neutral AT−$Au_8$ and GC−$Au_8$ complexes, the corresponding gold terminal atoms Au4 and Au8 gain large amounts of negative charges lying between −0.316 and −0.448 e, respectively (Tables 4 and 5). The gold atoms Au1 and Au5 that are bound to the N3 and N7 sites, respectively, of adenine and guanine in the neutral AT−$Au_8$ and GC−$Au_8$ complexes lose appreciable amounts of electronic charge lying between (−0.279 and −0.394 e). The clusters of gold atoms Au1−Au2−Au3−Au4 and Au5−Au6−Au7−Au8 located near the N3 and N7 sites of adenine and guanine in the neutral AT−$Au_8$ and GC−$Au_8$ complexes gain electronic charges lying between −0.244 and −0.336 e. The adenine and guanine moieties in the neutral AT−$Au_8$ and GC−$Au_8$ complexes are positively charged having lost large amounts of electronic charges, that is, about −0.49 and −0.58 e, respectively, and thus, these moieties attract the negatively charged gold clusters (Tables 4 and 5 and Figure 3). In the anionic AT−$Au_8$ complex, the excess negative charge is mainly localized on the Au1−Au2−Au3−Au4 cluster while in the anionic GC−$Au_8$ complex, it is localized on the Au5−Au6−Au7−Au8 cluster. Further, the negatively charged gold cluster Au1−Au2−Au3−Au4 in the anionic AT−$Au_8$ complex is located near the thymine moiety which is positively charged, carrying ∼0.27 e charge. In the anionic GC−$Au_8$ complex, the guanine moiety carries ∼0.4 e positive charge and thus it attracts the negatively charged cluster of gold atoms Au5−Au6−Au7−Au8.

**Electronic Isodensity Plots.** Plots of electronic isodensity surfaces of the HOMO and the LUMO of the neutral AT−$Au_8$

**TABLE 4: Mulliken Charges in Neutral and Anionic AT−$Au_8$ Complexes Calculated at the B3LYP/6-31+G**∪Lanl2DZ Level[a]**

| atom | AT−$Au_8$ (neutral) | | | AT−$Au_8$ (anion) | | |
|---|---|---|---|---|---|---|
| no. | adenine | thymine | gold | adenine | thymine | gold |
| 1 | −0.4535 | −0.4191 | 0.3483 | −0.4109 | −0.2371 | −0.4416 |
| 2 | 0.3054 | 0.6421 | −0.2054 | 0.3069 | 0.7451 | −0.2558 |
| 3 | −0.6464 | −0.5148 | −0.0709 | −0.6669 | −0.5717 | −0.2182 |
| 4 | 0.3204 | 0.1009 | −0.3155 | −0.4979 | −0.0117 | −0.3395 |
| 5 | 0.9997 | 0.8020 | 0.3015 | 0.6875 | 1.6844 | 0.3404 |
| 6 | −0.6468 | −0.3850 | −0.1762 | 0.4680 | −1.5569 | −0.2036 |
| 7 | −0.6599 | −0.5057 | −0.0368 | −0.3585 | −0.5559 | −0.0403 |
| 8 | 0.4955 | −0.4901 | −0.4097 | 0.1828 | −0.5015 | −0.4060 |
| 9 | −0.1764 | −0.6212 | | −0.2144 | −0.1203 | |
| 10 | −0.4079 | 0.1776 | | −0.6008 | 0.1568 | |
| 11 | 0.3410 | 0.1775 | | 0.3222 | 0.1568 | |
| 12 | 0.3929 | 0.1396 | | 0.4095 | 0.1786 | |
| 13 | 0.1862 | 0.1551 | | 0.1795 | 0.1874 | |
| 14 | 0.3374 | 0.3385 | | 0.3315 | 0.3341 | |
| 15 | 0.1925 | 0.3871 | | 0.1556 | 0.3824 | |
| Total | 0.5801 | −0.0155 | −0.5647 | 0.2941 | 0.2705 | −1.5646 |

[a] See Figures 1 and 3.

**TABLE 5: Mulliken Charges in Neutral and Anionic GC−$Au_8$ Complexes Obtained at the B3LYP/6-31+G**∪Lanl2DZ Level[a]**

| atom | GC−$Au_8$ (neutral) | | | GC−$Au_8$ (anion) | | |
|---|---|---|---|---|---|---|
| no. | guanine | cytosine | gold | guanine | cytosine | gold |
| 1 | −0.5286 | −0.3702 | 0.3937 | −0.5033 | −0.3824 | 0.4409 |
| 2 | 0.5546 | 0.6119 | −0.2188 | 0.3772 | 0.5772 | −0.2608 |
| 3 | −0.8032 | −0.5545 | 0.0192 | −0.4121 | −0.5553 | 0.0048 |
| 4 | 0.6425 | 0.0423 | −0.4480 | 1.1610 | 0.0627 | −0.4549 |
| 5 | 1.2726 | 0.2230 | 0.2791 | 0.5129 | 0.1869 | −0.3864 |
| 6 | −0.7885 | −0.2343 | −0.1845 | −0.7465 | −0.2257 | −0.1397 |
| 7 | −0.6716 | −0.5597 | −0.0413 | −0.6899 | −0.5434 | −0.1585 |
| 8 | 0.3605 | −0.4259 | −0.3888 | 0.3352 | −0.4441 | −0.4589 |
| 9 | −0.2219 | 0.4037 | | −0.2001 | 0.4152 | |
| 10 | −0.4460 | 0.3180 | | −0.5093 | 0.3113 | |
| 11 | −0.5069 | 0.1504 | | −0.5028 | 0.1368 | |
| 12 | 0.3816 | 0.1634 | | 0.3730 | 0.1470 | |
| 13 | 0.4041 | 0.3315 | | 0.3731 | 0.3230 | |
| 14 | 0.3217 | | | 0.3453 | | |
| 15 | 0.3331 | | | 0.3230 | | |
| 16 | 0.1857 | | | 0.1675 | | |
| Total | 0.4897 | 0.0996 | −0.5894 | 0.4042 | 0.0092 | −1.4135 |

[a] See Figures 2 and 3.

complex and that of the SOMO of the anionic AT−$Au_8$ complex are shown in Figure 4 while the corresponding plots for the neutral and anionic GC−$Au_8$ complexes are shown in Figure 5. In each of the neutral AT−$Au_8$ and GC−$Au_8$ complexes, the corresponding HOMO is localized on the Au1−Au4 cluster located near the N7 atom while the corresponding LUMO is localized on the Au5−Au8 cluster located near the N3 site of adenine or guanine. In the anionic AT−$Au_8$ complex, the SOMO is localized on the Au1−Au2−Au3−Au4 cluster located on the C5, C6, N1 side of thymine while in the anionic GC−$Au_8$ complex, the corresponding SOMO is localized on the Au5−Au6−Au7−Au8 cluster located on the C2, N3, C4, N9 side of guanine. Thus, while there is a similarity between the localizations of the HOMO and LUMO in the neutral AT−$Au_8$ and GC−$Au_8$ complexes, there is a clear difference between the localizations of the two SOMOs in this respect (Figures 4 and 5). From these plots, it is evident that if an electron is promoted from HOMO to LUMO in the neutral clusters, electron density will be transferred from the Au1−Au2−Au3−Au4 cluster located near the N7 site of adenine or guanine to the Au5−Au6−Au7−Au8 cluster located near the N3 site of the purines. The localizations of the SOMO in anionic AT−$Au_8$ and GC−$Au_8$ reveal an interesting difference between the two base pairs.

**TABLE 6: Adiabatic Electron Affinities (electronvolts) of Neutral AT−$Au_n$ and GC−$Au_n$ ($n$ = 4, 8) Complexes Obtained at the B3LYP/6-31+G**∪Lanl2DZ Level and Those of AT and GC Base Pairs in the Gas Phase and Hydrated Forms Obtained at Different Levels of Theory[a]**

| method | system | AEA[b] | AEA[c] |
|---|---|---|---|
| B3LYP/631+G**∪Lanl2DZ | AT−$Au_4$ | 1.78 (1.74) | 1.48 (1.60) |
| | AT−$Au_8$ | 2.47 (2.44) | 2.17 (2.30) |
| B3LYP/631+G**∪Lanl2DZ | GC−$Au_4$ | 1.84 (1.78) | 1.32 (1.40) |
| | GC−$Au_8$ | 2.18 (2.14) | 1.55 (1.76) |
| B3LYP/631+G**[d] | AT−$5H_2O$ | 0.97 (0.87) | 0.67 (0.72) |
| | AT−$13H_2O$ | 0.92 (0.73) | 0.62 (0.59) |
| BHLYP/DZP++[e] | AT | 0.13 (−0.02) | 0.11 (0.13) |
| | GC | 0.42 (0.28) | 0.56 (0.53) |
| B3LYP/DZP++[e] | AT | 0.36 (0.19) | 0.13 (0.16) |
| | GC | 0.60 (0.44) | 0.56 (0.53) |
| BP86/DZP++[e] | AT | 0.58 (0.41) | 0.26 (0.31) |
| | GC | 0.71 (0.54) | 0.58 (0.54) |
| B3P86/DZP++[e] | AT | 0.88 (0.72) | 0.14 (0.18) |
| | GC | 1.15 (0.99) | 0.61 (0.57) |
| B3LYP/TZ2P++[e,f] | AT | 0.31 (0.15) | 0.13 (0.16) |
| | GC | 0.48 (0.37) | 0.51 (0.31) |

[a] Uncorrected AEAs are given in parentheses. [b] AEA calculated using eq 1. [c] AEA calculated using eq 3. [d] Reference 22b. [e] Reference 17c. [f] B3LYP/TZ2P++ single-point calculation at structure optimized using the DZP++ basis set (ref 17c).

Regarding the possible use of gold clusters as a molecular wire, a study has been recently carried out by Marx, Parrinello, and co-workers[28] using the Car−Parrinello ab initio molecular dynamics method. In their study, they demonstrated that a thiolate molecule anchored on a stepped gold surface leads to the formation of a monatomic gold nanowire, which is followed by the breaking of an Au−Au bond.[28] The pulled gold atoms from the gold surface adopted a zigzag structure, with the Au−Au distances lying in the range 2.6−2.9 Å, which finally results in the formation of a triatomic gold wire.[28] The wire thus formed remained stable up to the distance of 11 Å. Our optimized clusters of gold atoms bound to the DNA base pairs show some characteristic features, for example, zigzag and triangular structures that are similar to those found by Marx et al.[28] These results indicate the possibility of using gold clusters bound to DNA as molecular wires in DNA-based devices.

**Adiabatic Electron Affinity.** The charge-transfer process in DNA is of fundamental importance from many technological points of view.[10,11] The study of adiabatic electron affinities (AEAs) can provide valuable information about the occurrence of charge-transfer phenomena involving different molecules and complexes. Theoretically, the AEA of a molecule is calculated as the difference between the total energies ($T$) of a molecule in its optimized neutral and anionic forms. Thus

$$\mathrm{AEA} = T^{\mathrm{neutral}} - T^{\mathrm{anion}} \quad (1)$$

The AEA of a molecule or complex can also be obtained as the difference of enthalpies ($\Delta H$) of formation of an anion and that of the corresponding neutral molecule.[50] Recently, it has been shown that AEAs of hydrogen bonded complexes AB of molecules A and B can be successfully calculated using the enthalpies of formation of optimized neutral AB and its anion using eq 1 without including thermal correction.[22]

Thus, as discussed earlier,[22] the AEAs are given as

$$\mathrm{AEA} = \Delta E^{\mathrm{AB}} - \Delta E^{\mathrm{AB}^-} \quad (2)$$

where $\Delta E^{\mathrm{AB}}$ and $\Delta E^{\mathrm{AB}^-}$ are the binding or dissociation energies

of the neutral and anionic forms of AB, respectively. In eq 2, it is assumed that B is more electronegative than A. Thus, in $AB^-$, the excess electronic charge is assumed to be localized on B. In the present study, we calculated the AEAs of AT−$Au_n$ and GC−$Au_n$ ($n$ = 4, 8) complexes using eq 2. Equation 2 in expanded form is

$$\mathrm{AEA} = (T^{(\mathrm{AB-Au}_n)} - (T^{\mathrm{AB}} + nT^{\mathrm{Au}})) - (T^{(\mathrm{AB-Au}_n)^-} - (T^{\mathrm{AB}^-} + nT^{\mathrm{Au}})) \quad (3)$$

In eq 3, $T^{(\mathrm{AB-Au}_n)}$ and $T^{(\mathrm{AB-Au}_n)^-}$ are the total energies of neutral and anionic AB−$Au_n$ complexes, where AB corresponds to an AT or GC base pair. $T^{\mathrm{AB}}$ is the total energy of AB, and $T^{\mathrm{Au}}$ is the total energy of a neutral gold atom. By the use of eqs 1 and 3, the AEAs of AT−$Au_n$ and GC−$Au_n$ ($n$ = 4, 8) were evaluated and the results obtained are presented in Table 6 along with the AEAs of the AT and GC base pairs in their gas phase and hydrated environment using different methods.

The zero-point energy-corrected AEAs of the AT−$Au_n$ and GC−$Au_n$ ($n$ = 4, 8) complexes obtained using the B3LYP/6-31+G**∪Lanl2DZ level of theory and eq 1 lie in the ranges 1.78−2.47 while the corresponding uncorrected AEAs lie in the ranges 1.74−2.44 eV. Whereas the corresponding AEAs obtained using eq 3 lie in the ranges 1.48−2.17 and 1.40−2.30 eV, respectively (Table 6). Thus, we find that the complexes of the AT and GC base pairs with gold clusters have appreciably larger AEAs than the isolated base pairs (Table 6).

## Conclusion

We arrive at the following conclusions from the present study:

1. In the neutral AT−$Au_n$ and GC−$Au_n$ ($n$ = 4, 8) complexes, the gold clusters bind near the N3 and N7 sites of adenine and guanine where, when $n$ = 8, the gold atoms make a T-shaped structure in each case. In these complexes, thymine and cytosine are not preferred for binding by the gold clusters. The present results are in a satisfactory agreement with those obtained earlier by other authors.

2. When going from neutral to anionic AT−$Au_n$ and GC−$Au_n$ ($n$ = 4, 8) complexes, binding patterns of gold clusters are appreciably modified and these modifications are different for the two base pairs. Thus, when going from the neutral AT−$Au_8$ to the corresponding anionic complex, the cluster of four gold atoms located near the N7 site of adenine gets shifted to near the C5, C6, N1 side of thymine. However, when going from the neutral GC−$Au_8$ complex to the corresponding anionic complex, only the shape of the cluster of four gold atoms located near the N3 site of guanine is modified from one of T-shape to one of zigzag type.

3. In the AT−$Au_8$ or GC−$Au_8$ neutral complex, the HOMO and LUMO are localized near the N3 and N7 sites of guanine or adenine on the gold clusters, respectively. The SOMO in the anionic AT−$Au_8$ complex is localized near the C5, C6, N1 atoms of thymine on the gold clusters while the SOMO of the anionic GC−$Au_8$ complex is localized near the N11, N3, C4, N9 atoms of guanine on the gold clusters.

4. There are appreciable amounts of charge transfer from the AT and GC base pairs to the gold clusters in the corresponding neutral AT−$Au_n$ and GC−$Au_n$ ($n$ = 4, 8) complexes. In each of the anionic complexes, the excess negative charge is localized on the gold clusters to which some more negative charge is also transferred from the bases.

5. The AEAs of the AT and GC base pairs increased substantially when complexed with gold atoms in comparison to their gas phase and hydrated complexes.

**Acknowledgment.** The present work was mainly carried out at the German Cancer Research Center (DKFZ), Heidelberg, and it was partly carried out at the Banaras Hindu University. A.K. thanks DKFZ for a visiting scientist fellowship. He also thanks Dr. Michaela Knapp-Mohammady and Ms. A. Retzmann for their cooperation. P.C.M. thanks the Council of Scientific and Industrial Research, New Delhi, and the University Grants Commission, New Delhi, for financial support.

## References and Notes

(1) Watson, J. D.; Crick, F. H. C. *Nature* **1953**, *171*, 737.

(2) (a) Hwang, J. S.; Hong, S. H.; Kim, H. K.; Kwon, Y. W.; Jin, J. I.; Hwang, S. W.; Ahn, D. *Extended Abstracts of the 2004 international conference on solid-state devices and materials*; Tokyo, Japan, 2004; p 332. (b) Yan, H.; Zhang, X.; Shen, Z.; Seeman, N. C. *Nature* **2002**, *415*, 62. (c) Mao, C.; Sun, W.; Shen, Z.; Seeman, N. C. *Nature* **1999**, *397*, 144. (d) Wettig, S. D.; Li, C.-Z.; Long, Y.-T.; Kraatz, H.-B.; Lee, J. *Anal. Sci.* **2003**, *19*, 23. (e) Simmel, F. C.; Dittmer, W. U. *Small* **2005**, *1*, 284.

(3) Braun, E.; Eichen, Y.; Sivan, U.; Ben-Yoseph, G. *Nature* **1998**, *391*, 775.

(4) Richter, J.; Mertig, M.; Pompe, W.; Monch, I.; Schackert, H. K. *Appl. Phys. Lett.* **2001**, *78*, 536.

(5) (a) Adessi, Ch.; Walch, S.; Anantram, M. P. *Phys. Rev. B* **2003**, *67*, 081405. (b) Heath, J. R.; Ratner, M. A. *Phys. Today* **2003**, 43. (c) Long, Yi-T.; Li, C.-Z.; Kraatz, H.-B.; Lee, J. S. *Biophys. J.* **2003**, *84*, 3218. (d) Moreno-Herrero, F.; Herrero, P.; Moreno, F.; Colchero, J.; Gómez-Navarro, C.; Gómez-Herrero, J.; Baró, A. M. *Nanotechnology* **2003**, *14*, 128.

(6) Sun, Y.; Harris, N. C.; Kiang, C.-H. *Physica A* **2005**, *350*, 89.

(7) (a) Mirkin, C. A.; Lestsinger, R. L.; Mucic, R. C.; Storhoff, J. J. *Nature* **1996**, *382*, 607. (b) Elghanian, R.; Storhoff, J. J.; Mucic, R. C.; Letsinger, R. L.; Mirkin, C. A. *Science* **1997**, *277*, 1078.

(8) (a) Kiang, C.-H. *Physica A* **2003**, *321*, 164. (b) Ventra, M. D.; Zwolak, M. In *Encyclopedia of Nanoscience and Nanotechnology*; Nalwa, H. S., Ed.; American Scientific Publishers: Stevenson Ranch, CA, 2004; Vol. X, pp 1−19.

(9) (a) Hou, S.; Zhang, J.; Li, R.; Ning, J.; Han, R.; Shen, Z.; Zhao, X.; Xue, Z.; Wu, Q. *Nanotechnology* **2005**, *16*, 239. (b) Reed, M. A.; Zhou, C.; Miller, C. J.; Burgin, T. P.; Tour, J. M. *Science* **1997**, *278*, 252. (c) DiVenta, M.; Pantelides, S. T.; Lang, N. D. *Phys. Rev. Lett.* **2000**, *84*, 979. (d) Derosa, P. A.; Seminario, J. M. *J. Phys. Chem. B* **2001**, *105*, 471. (e) Xue, Y.; Ratner, M. A. *Phys. Rev. B* **2003**, *68*, 115407.

(10) (a) Cai, Z.; Sevilla, M. D. *Dalton Res.* **2003**, *159*, 411. (b) Giese, B. *Acc. Chem. Res.* **2000**, *33*, 631. (c) Yang, X.; Wang, X.-B.; Vorpagel, E. R.; Wang, L.-S. *Proc. Natl. Acad. Sci.* **2004**, *101*, 17588.

(11) Giese, B.; Amaudrut, J.; Köhler, A.-K.; Spormann, M.; Wessely, S. *Nature* **2001**, *412*, 318.

(12) Schiedt, J.; Weinkauf, R.; Neumark, D. M.; Schlag, E. W. *Chem. Phys.* **1998**, *239*, 511.

(13) Wetmore, S. D.; Boyd, R. J.; Eriksson, L. A. *Chem. Phys. Lett.* **2000**, *322*, 129.

(14) (a) Oyler, N. A.; Adamowicz, L. *J. Phys. Chem.* **1993**, *97*, 1122. (b) Desfrancois, C.; Abdoul-Carime, H.; Carles, S.; Periquet, V.; Schermann, J. P.; Smith, D. M. A.; Adamowicz, L. *J. Chem. Phys.* **1999**, *110*, 11876. (c) Smets, J.; Smith, D. M. A.; Elkadi, Y.; Adamowicz, L. *J. Phys. Chem. A* **1997**, *101*, 9152. (d) Smets, J.; Jalbout, A. F.; Adamowicz, L. *Chem. Phys. Lett.* **2001**, *342*, 342.

(15) (a) Hendricks, J. H.; Lyapustina, S. A.; deClercq, H. L.; Snodgrass, J. T.; Bowen, K. H. *J. Chem. Phys.* **1996**, *104*, 7788. (b) Hendricks, J. H.; Lyapustina, S. A.; deClercq, H. L.; Bowen, K. H. *J. Chem. Phys.* **1998**, *108*, 8.

(16) (a) Barnett, R. N.; Cleveland, C. L.; Joy, A.; Landman, U.; Schuster, G. B. *Science* **2001**, *294*, 567. (b) Barnett, R. N.; Cleveland, C. L.; Landman, U.; Bonne, E.; Kanvah, S.; Schuster, G. B. *J. Phys. Chem. A* **2003**, *107*, 3525.

(17) (a) Wesolowski, S. S.; Leininger, M. L.; Pentchev, P. N.; Schaefer, H. F., III. *J. Am. Chem. Soc.* **2001**, *123*, 4023. (b) Richardson, N. A.; Wesolowski, S. S.; Schaefer, H. F., III. *J. Am. Chem. Soc.* **2002**, *124*, 10163. (c) Richardson, N. A.; Wesolowski, S. S.; Schaefer, H. F., III. *J. Phys. Chem. B* **2003**, *107*, 848. (d) Gu, J.; Xie, Y.; Schaefer, H. F., III. *J. Phys. Chem. B* **2005**, *109*, 13067.

(18) Wiley, J. R.; Robinson, J. M.; Ehdaie, S.; Chen, E. C. M.; Chen, E. S. D.; Wentworth, W. E. *Biochem. Biophys. Res. Commun.* **1991**, *180*, 841.

(19) (a) Chen, E. S. D.; Chen, E. C. M.; Sane, N. *Biochem. Biophys. Res. Commun.* **1998**, *246*, 228. (b) Chen, E. C. M.; Chen, E. S. D. *J. Phys. Chem B* **2000**, *104*, 7835. (c) Chen, E. S. D.; Chen, E. C. M. *Bioelectrochem. Bioenergetics* **1998**, *46*, 15.

(20) (a) Li, X.; Cai, Z.; Sevilla, M. D. *J. Phys. Chem. A* **2002**, *106*, 1596. (b) Li, X.; Cai, Z.; Sevilla, M. D. *J. Phys. Chem. A* **2002**, *106*, 9345. (c) Li, X.; Cai, Z.; Sevilla, M. D. *J. Phys. Chem. B* **2001**, *105*, 10115.

(21) Radisic, D.; Bowen, K. H., Jr.; Dabkowska, I.; Storoniak, P.; Rak, J.; Gutowski, M. *J. Am. Chem. Soc.* **2005**, *127*, 6443.

(22) (a) Kumar, A.; Knapp-Mohammady, M.; Mishra, P. C.; Suhai, S. *J. Comput. Chem.* **2004**, *25*, 1047. (b) Kumar, A.; Mishra, P. C.; Suhai, S. *J. Phys. Chem. A* **2005**, *109*, 3971. (c) To be published.

(23) Seeman, N. C. *Chem. Biol.* **2003**, *10*, 1151.

(24) Endres, R. G.; Cox, D. L.; Singh, R. R. P. *Rev. Mod. Phys.* **2004**, *76*, 195.

(25) Gomes, J. R. B.; Illas, F. *Int. J. Mol. Sci.* **2001**, *2*, 211.

(26) (a) Yanov, I.; Leszczynski, J. *Int. J. Quantum Chem.* **2004**, *96*, 2004. (b) Burda, J. V.; Leszczynski, J. *Inorg. Chem.* **2003**, *42*, 7162.

(27) Kimura-Suda, H.; Petrovykh, D. Y.; Tarlov, M. J.; Whitman, L. J. *J. Am. Chem. Soc.* **2003**, *125*, 9014.

(28) Krüger, D.; Fuchs, H.; Rousseau, R.; Marx, D.; Parrinello, M. *Phys. Rev. Lett.* **2002**, *89*, 186402.

(29) Liu, C.; Walter, D.; Neuhauser, D.; Baer, R. *J. Am. Chem. Soc.* **2003**, *125*, 13936.

(30) Haglmüller, J.; Rauter, H.; Bauer, G.; Pittner, F.; Schalkhammer, T. *IEE Proc.: Nanobiotechnol.* **2005**, *152*, 53.

(31) LaBean, T. H. In *Computational Biology and Genome Informatics*; Wang, J. T. L., Wu, C. H., Wang, P. P., Eds.; World Scientific Publishing: Singapore, 2003; Chapter 2.

(32) Jang, N. H. *Bull. Korean Chem. Soc.* **2002**, *23*, 1790.

(33) Östblom, M.; Liedberg, B.; Demers, L. M.; Mirkin, C. A. *J. Phys. Chem. B* **2005**, *109*, 15150.

(34) (a) Kryachko, E. S.; Remacle, F. *Nano Lett.* **2005**, *5*, 735. (b) Kryachko, E. S.; Remacle, F. *J. Phys. Chem. B* **2005**, *109*, 22746.

(35) (a) Lopez, N.; Janssens, T. V. W.; Clausen, B. S.; Xu, Y.; Mavrikakis, M.; Bligaard, T.; Nørskov, J. K. *J. Catal.* **2004**, *223*, 232. (b) Lemire, C.; Meyer, R.; Shaikhutdinov, S.; Freund, H.-J. *Angew. Chem., Int. Ed.* **2004**, *43*, 118. (c) Lopez, N.; Nørskov, J. K.; Janssens, T. V. W.; Carlsson, A.; Puig-Molina, A.; Clausen, B. S.; Grunwaldt, J.-D. *J. Catal.* **2004**, *225*, 86. (d) Liu, Z.-P.; Jenkins, S. J.; King, D. A. *Phys. Rev. Lett.* **2005**, *94*, 196102.

(36) Becke, A. D. *J. Chem. Phys.* **1993**, *98*, 1372.

(37) Stephen, P. J.; Devlin, F. J.; Frisch, M. J.; Chabalowski, C. F. *J. Phys. Chem.* **1994**, *98*, 11623.

(38) Lee, C.; Yang, W.; Parr, R. G. *Phys. Rev. B* **1988**, *37*, 785.

(39) (a) Hay, P. J.; Wadt, W. R. *J. Chem. Phys. Chem.* **1985**, *82*, 270. (b) Wadt, W. R.; Hay, P. J. *J. Chem. Phys. Chem.* **1985**, *82*, 284. (c) Hay, P. J.; Wadt, W. R. *J. Chem. Phys. Chem.* **1985**, *82*, 299.

(40) Frisch, M. J.; Trucks, G. W.; Schlegel, H. B.; Scuseria, G. E.; Robb, M. A.; Cheeseman, J. R.; Montgomery, J. A., Jr.; Vreven, T.; Kudin, K. N.; Burant, J. C.; Millam, J. M.; Iyengar, S. S.; Tomasi, J.; Barone, V.; Mennucci, B.; Cossi, M.; Scalmani, G.; Rega, N.; Petersson, G. A.; Nakatsuji, H.; Hada, M.; Ehara, M.; Toyota, K.; Fukuda, R.; Hasegawa, J.; Ishida, M.; Nakajima, T.; Honda, Y.; Kitao, O.; Nakai, H.; Klene, M.; Li, X.; Knox, J. E.; Hratchian, H. P.; Cross, J. B.; Adamo, C.; Jaramillo, J.; Gomperts, R.; Stratmann, R. E.; Yazyev, O.; Austin, A. J.; Cammi, R.; Pomelli, C.; Ochterski, J. W.; Ayala, P. Y.; Morokuma, K.; Voth, G. A.; Salvador, P.; Dannenberg, J. J.; Zakrzewski, V. G.; Dapprich, S.; Daniels, A. D.; Strain, M. C.; Farkas, O.; Malick, D. K.; Rabuck, A. D.; Raghavachari, K.; Foresman, J. B.; Ortiz, J. V.; Cui, Q.; Baboul, A. G.; Clifford, S.; Cioslowski, J.; Stefanov, B. B.; Liu, G.; Liashenko, A.; Piskorz, P.; Komaromi, I.; Martin, R. L.; Fox, D. J.; Keith, T.; Al-Laham, M. A.; Peng, C. Y.; Nanayakkara, A.; Challacombe, M.; Gill, P. M. W.; Johnson, B.; Chen, W.; Wong, M. W.; Gonzalez, C.; Pople, J. A. *Gaussian 03*, Revision B.04; Gaussian, Inc.: Pittsburgh, PA, 2003.

(41) *GaussView*, Gaussian, Inc.: Pittsburgh, PA, 2003.

(42) Kennard, O.; Hunter, W. N. *Angew. Chem., Int. Ed. Engl.* **1991**, *30*, 1254.

(43) Wahl, C.; Sundarralingham, M. *Biopolymers* **1997**, *44*, 45.

(44) Seeman, N. C.; Rosenberg, J. M.; Suddath, F. L.; Kim, J. J. P.; Rich, A. *J. Mol. Biol.* **1976**, *104*, 109.

(45) Rosenberg, J. M.; Seeman, N. C.; Day, R. O.; Rich, A. *J. Mol. Biol.* **1976**, *104*, 145.

(46) Kurita, N. K.; Danilov, V. I.; Anisimov, V. M. *Chem. Phys. Lett.* **2005**, *404*, 164.

(47) Tao, N. J.; de Rose, J. A.; Lindsay, S. M. *J. Phys. Chem.* **1993**, *97*, 910.

(48) Giese, B.; McNaughton, D. *Phys. Chem. Chem. Phys.* **2002**, *4*, 5171.

(49) Häkkinen, H.; Moseler, M.; Landman, U. *Phys. Rev. Lett.* **2002**, *89*, 33401.

(50) Rienstra-Kiracofe, J. C.; Tschumper, G. S.; Schaefer, H. F., III; Nandi, S.; Ellison, G. B. *Chem. Rev.* **2002**, *102*, 231.